

# APPLICATION OF THE FOURIER-BESSEL TRANSFORMATION FOR THE NUMERICAL SOLUTION OF THE EQUATIONS OF NONLINEAR OPTICS

V.L. Derbov, Yu.N. Ponomarev, and S.K. Potapov

*Saratov State University  
Institute of Atmospheric Optics,  
Siberian Branch of the USSR Academy of Sciences, Tomsk  
Received October 4, 1988*

*An improved scheme for performing a fast Fourier-Bessel transformation for the radially symmetric wave equation describing the nonlinear propagation of light is proposed. The propagation of a strong light beam in a transparent nonuniform medium with a cubic nonlinearity is calculated.*

## INTRODUCTION

The development of numerical methods for calculating the equations of nonlinear optics was motivated by the development of laser technology and the widespread use of this technology in the solution of the problems arising in the remote diagnostics of a medium. When strong laser radiation propagates in matter the characteristics of the matter in the propagation channel change. Thus, for example, in the problems of atmospheric optics the nonlinear correction to the refractive index, whose magnitude is determined by the contributions from molecular and aerosol components of the air and depends in a complicated manner on the character of the interaction with optical radiation (resonance, nonstationariness) and the uniformity of the medium, must be taken into account.

The behavior of the characteristics of strong optical radiation along extended nonlinear paths is described best by algorithms based on conservative difference schemes.<sup>1,2</sup> For arbitrary nonlinearity, however, there does not exist a universal technique for constructing conservative schemes. Moreover, in the case of implicit schemes questions regarding the convergence of the nonlinear system of equations obtained arise.

In the last few years, to describe the propagation of axisymmetric beams, the nonlinear wave equation has been solved with the help of the Fourier-Bessel transformation,<sup>3-5</sup> the analog of the Fourier transformation for one-dimensional wave equations. The efficiency of pseudospectral methods was demonstrated in Ref. 6 for the example of a finite Fourier transformation for the solution of nonlinear wave problems. The numerical algorithm described in Ref. 6 is distinguished by the features that it includes a specific technique which enables taking into account correctly the higher order harmonics of the pseudospectral transformation and the difference scheme for the slow variable is an explicit scheme. The latter property makes the method of Ref. 6 very flexible and versatile, and it makes it possible to transfer the basic algorithm to the

systems of equations with arbitrary nonlinearity. Although the indicated method is not absolutely stable, it nonetheless makes it possible to perform practical calculations with an acceptably small step.

Successful examples of the application<sup>5</sup> of the fast Fourier-Bessel transformation algorithm<sup>3</sup> motivated us to construct a computational scheme of the type described in Ref. 6 with an improvement of the algorithm of Ref. 3 for radially symmetric nonlinear wave equations.

## DESCRIPTION OF THE ALGORITHM

The starting equation has the form

$$i \frac{\partial E}{\partial z} + \left[ \frac{\partial^2}{\partial r^2} + \frac{1}{r} \frac{\partial}{\partial r} \right] E = P \exp(i \Delta k \cdot z), \quad (1)$$

where  $P$  is an arbitrary function of the complex field  $\varepsilon$ . Equation (1) can also be one of the equations of the system describing the interaction of waves in a nonlinear medium.

Let us apply, as done in Refs. 3-5, to (1) the Fourier-Bessel transformation

$$E(\rho, z) \equiv \hat{B}E(r, z) = \int_0^\infty r dr I_0(\rho r) E(r, z), \quad (2)$$

whose inverse has the same form<sup>7</sup>

$$E(r, z) \equiv \hat{B}^{-1}(E(\rho, z)) = \int_0^\infty \rho d\rho I_0(\rho r) E(\rho, z), \quad (3)$$

where  $J_0$  is a Bessel function of the first kind. The Fourier-Bessel transformation has the following important property:<sup>7</sup>

$$\hat{B} \left[ \frac{\partial^2 E}{\partial r^2} + \frac{1}{r} \frac{\partial E}{\partial r} \right] = -\rho^2 \hat{B}E. \quad (4)$$

It enables reducing (1) to an ordinary differential equation for the transform

$$\left(i\frac{\partial}{\partial z} - \rho^2\right)\hat{B}E = \hat{B}P\exp(i\Delta k \cdot z), \tag{5}$$

We shall solve (5) numerically with the help of the ideas contained in Ref. 6 which permit taking into account correctly the contribution of the higher harmonics ( $\rho \rightarrow \infty$ ) of the transformation (2). The following difference equation is the discrete analog of Eq. (5):

$$\hat{B}E(z+\Delta z) - \hat{B}E(z) = -i\Delta z \left\{ \rho^2 \hat{B} \left[ \frac{3}{2}E(z) - \frac{1}{2}E(z-\Delta z) \right] - \frac{3}{2}\hat{B}P^z \exp(i\Delta k \cdot z) + \frac{1}{2}\hat{B}P(z-\Delta z) \exp(i\Delta k(z-\Delta z)) \right\}, \tag{6}$$

constructed using the Adams-Bachfort scheme. For large values of  $\rho$  a small error in calculating  $\hat{B}E$  may result in a significant error in determining  $E(z + \Delta z)$ ; in the process the quantity  $\hat{B}P$  approaches zero, and Eqs. (5) and (6) assume asymptotically the following form:

$$\left(i\frac{\partial}{\partial z} - \rho^2\right)\hat{B}E = 0; \tag{7}$$

$$\hat{B}E(z+\Delta z) - \hat{B}E(z) = -i\Delta z \rho^2 \hat{B} \left[ \frac{3}{2}E(z) - \frac{1}{2}E(z-\Delta z) \right]. \tag{8}$$

Following Ref. (6) we replace in (6) and (8) the quantity  $\rho^2\Delta z$  by the correction function  $\varphi(\Delta z, \rho)$ , which is sought from the condition that (8) be the exact discrete analog of Eq. (7):

$$\hat{B}E(z+\Delta z) - \hat{B}E(z) = -i\varphi(\Delta z, \rho) \hat{B} \left[ \frac{3}{2}E(z) - \frac{1}{2}E(z-\Delta z) \right]. \tag{9}$$

Solving Eq. (7) we obtain

$$\hat{B}E(z+\Delta z) = \hat{B}E(z) \exp(-i\rho^2\Delta z). \tag{10}$$

Substituting (10) into (9) we obtain an equation for the correction function  $\varphi(\Delta z, \rho)$ , whose solution has the form

$$\varphi(\Delta z, \rho) = 2i \frac{\exp(-i\rho^2\Delta z) - 1}{3 - \exp(i\rho^2\Delta z)}. \tag{11}$$

We note that for  $\Delta z\rho^2 \ll 1$  the equality  $\varphi(\Delta z, \rho) \approx \Delta z\rho^2$  holds to within second order-terms. For this reason the difference scheme

$$\hat{B}E(z+\Delta z) - \hat{B}E(z) = -i \left\{ \varphi(\Delta z, \rho) \hat{B} \left[ \frac{3}{2}E(z) - \frac{1}{2}E(z-\Delta z) \right] - \Delta z \left[ \frac{3}{2}\hat{B}P(z) \exp(i\Delta kz) - \frac{1}{2}\hat{B}P(z-\Delta z) \exp(i\Delta k(z-\Delta z)) \right] \right\} \tag{12}$$

gives the same accuracy of approximation as the Adams-Bachfort scheme,  $O(\Delta z^2)$ , and it also makes it possible to avoid the increase in error for large values of  $\rho$ . Applying to Eq. (12) the inverse Fourier-Bessel transformation we obtain the basic equation employed in the further calculations:

$$E(z+\Delta z) = E(z) - i\hat{B}^{-1}\varphi(\Delta z, \rho)\hat{B} \left[ \frac{3}{2}E(z) - \frac{1}{2}E(z-\Delta z) \right] + i\Delta z \left[ \frac{3}{2}P(z) \exp(i\Delta kz) - \frac{1}{2}P(z-\Delta z) \exp(i\Delta k(z-\Delta z)) \right]. \tag{13}$$

### NUMERICAL IMPLEMENTATION OF THE FOURIER-BESSEL TRANSFORMATION

As one can see from Eq. (13), to calculate the field the Fourier-Bessel transformation must be performed twice at each step in  $z$ . When the integral is approximated directly by a sum this procedure is very time consuming; the number of arithmetic operations required is proportional to  $N^2$ , where  $N$  is the number of nodes in the discrete approximation of the integral (2). In Ref. 3 Siegman reduced, with the help of Gardner's substitution of variables, the integral (2) to a sum which is calculated with the help of the fast Fourier transform. Thus the number of operations becomes proportional to  $N \ln N$ . In Ref. 3, however, the approximation of the integral (2) is very rough and cannot be used to solve Eq. (1) numerically when the Fourier-Bessel transformation is employed repeatedly. We modified Siegman's computational scheme by using special techniques to integrate rapidly oscillating functions numerically.

We choose a discrete set of values  $r_n$  and  $\rho_m$ :

$$\begin{aligned} r_0 &= 0 \text{ at } n=0; \quad \rho_0 = 0 \text{ at } m=0; \\ r_n &= r_1 e^{\alpha(n-1)}, \text{ at } n=1, 2, \dots, N; \quad \rho_m = \rho_1 e^{\alpha(m-1)}, \\ &\text{at } m=1, 2, \dots, N. \end{aligned} \tag{14}$$

The integral (2) can be represented as a sum

$$E(\rho, z) = \sum_{n=0}^{N-1} \int_{r_n}^{r_{n+1}} r dr I_0(\rho r) E(r, z). \tag{15}$$

The upper limit of the integral in Eq. (15) is chosen to be finite but quite large; such a choice can always be made, if the field  $\varepsilon(r, z)$  decreases as  $\rho \rightarrow \infty$ , which is a natural condition for real beams.

We shall assume that the slowly varying function  $E(r, z)$  is constant on each segment of the integration:

$$E(\rho, z) \approx \bar{E}_n; \quad r_n \leq r \leq r_{n+1}. \tag{16}$$

Then the integrals in (15) can be calculated analytically, and the following sum is obtained:

$$E(\rho, z) = \sum_{n=0}^{N-1} \bar{E}_n \frac{1}{\rho} \left[ r_{n+1} I_1(\rho r_{n+1}) - r_n I_1(\rho r_n) \right], \quad (17)$$

which it is more convenient to transform into the form

$$E(\rho_m, z) = \frac{1}{\rho_m} \sum_{n=1}^N (\bar{E}_{n-1} - \bar{E}_n) r_n. \quad (18)$$

To accelerate the computation of the sum (18) we employed a fast Fourier transform algorithm that is identical to the one employed in Ref. 3, making the assumption that

$$\bar{E}_n = [E(r_{n+1}, z) + E(r_n, z)]/2, \quad (19)$$

though these terms can also be defined differently.

### EXAMPLES OF APPLICATIONS

As an example we shall study the propagation of a light beam in a transparent nonuniform medium with a cubic nonlinearity. In this case, the main equation (13) assumes the form (see, for example, Ref. 5):

$$\begin{aligned} E(z+\Delta z) = & E(z) - i\hat{B}^{-1}\varphi(\Delta z, \rho)\hat{B}\left[\frac{3}{2}E(z) - \frac{1}{2}E(z-\Delta z)\right] + \\ & + i\Delta z\left\{V^2U(r)\left[\frac{3}{2}E(z) - \frac{1}{2}E(z-\Delta z)\right] + 2R\left[\frac{3}{2}|E(z)|^2E(z) - \right. \right. \\ & \left. \left. - \frac{1}{2}|E(z-\Delta z)|^2E(z-\Delta z)\right]\right\}, \quad (20) \end{aligned}$$

where  $V = kw_0(N_c^2 - N_0^2)^{1/2} / N_0$ ;  $k$  is the wave number;  $w_0$  is the characteristic radius of the nonuniformity;  $R = L_d/L_{nl}$ ; where  $L_d$  is the diffraction length and  $L_{nl}$  is the length of the nonlinearity,

$$L_{nl} = \frac{n_0}{2kn_2|E_0|^2}, \quad (21)$$

$n_c$  and  $n_0$  are the values of the refractive index at the center ( $r = 0$ ) and at the periphery ( $r = \infty$ ) of the nonuniformity of the medium; the function  $U(r)$  determines the profile of the nonuniformity;  $N_2|E_0|^2$  is the nonlinear correction to the refraction index; and,  $\epsilon_0$  is the initial value of the amplitude of the field on the  $z$  axis. With this definition of  $R$  the quantity  $E$  in Eq. (20) is measured in units of  $|E_0|$ . The choice of the parameters  $r_1$ ,  $\alpha$ , and  $N$  is largely arbitrary, but in order to ensure that the boundary conditions are satisfied in the limit  $r \rightarrow \infty$  the field  $E(r, z)$  at the points  $r_n$  with  $n$  close to  $N$  must be quite small in absolute magnitude. In addition, near the axis of the beam the step in  $r$  must be small enough so that the details of the profile of the field are reproduced. We employed  $r_1 = 0.08$ ,  $\alpha = 0.03$ , and  $N = 128$ , which

values were chosen by an empirical method. The same values of the parameters were also employed to construct a grid in the space of the variable.

The input data for the program were as follows:

1) the parameters of the discrete coordinate grid  $r_1$ ,  $\rho_1$ ,  $\alpha$ ,  $N$ , and  $\Delta z$  as well as the starting and final values of  $z$ ; 2) the profile of the field intensity  $E(z = 0)$  at the start of the medium; 3) the profile of the refractive index of the medium  $U(r)$ ; and, 4) the coefficients  $V$  and  $R$ , characterizing, respectively, the depth of the profile of the nonuniformity of the medium and the magnitude of the cubic nonlinearity. The parameter  $R$  is actually determined by the strength of the beam at the start. At each step in  $z$  the program computes a discrete set of values of the real and imaginary parts of the amplitude of the electric field  $E(r, z)$  according to Eq. (20). To describe the profile of the field quantitatively and monitor the calculations the total power

$$W = \int_0^\infty r dr |E|^2 \quad (22)$$

and the cross section of the beam scaled to the intensity

$$\sigma^2 = \int_0^\infty r dr r^2 |E|^2 / W \quad (23)$$

were printed out at each point  $z$  of interest. The integrals in (24) and (25) were calculated using the trapezoidal rule.

The propagation of a beam with an initial gaussian field profile

$$E(z=0) = \exp(-\eta_0 r^2) \quad (24)$$

and a starting plane wavefront was studied as a function of  $V$  and  $R$  in a medium with a gaussian  $U = \exp(-r^2)$  and hypergaussian  $U = \exp(-r^6)$  profiles of the nonuniformity. For numerical convenience the value  $\eta_0 = \pi_0$  was chosen; this made it possible to employ the same discrete coordinate grid in  $r$  all cases.

#### 1. Nonuniformity with a gaussian profile.

Figure 1 shows the computed beam cross sections scaled to the starting value as a function of the dimensionless coordinate  $z$  measured in diffraction lengths. For  $V = 0$  (a uniform linear medium) free diffraction of the beam is obtained (curve 1); in accordance with the well-known analytical solution this doubles the cross section at a distance of  $1/\eta_0$  from the start. For  $V = \eta_0$  a weak nonuniformity of the medium slows down the divergence somewhat (curve 2). For  $V = 2\eta_0$  (curve 3) "trapping" of the beam, whose cross section starts to oscillate, occurs; this is a natural result of the simultaneous manifestation of focusing and diffraction. As  $V$  is further increased the period of the oscillations decreases approximately linearly, and the phase is reversed, since for large  $V$  and small  $z$  the focusing

starts to predominate over diffraction. Of the values studied  $V = 2.3 \eta_0$  (curve 5) is closest to the case when the input field is almost identical to the fundamental characteristics mode of the medium.

Figure 2 illustrates the effect of nonlinearity on the propagation of a beam close to the characteristic mode ( $V = 2.3 \eta_0$ ). One can see that as  $R$  increases the focusing action of the nonuniform medium increases, the amplitude of the oscillation of the beam cross section increases, and at the same time the period of these oscillations remains practically constant. In the case of high intensities ( $R = 5$ ) a beam which, being weak, would propagate in an almost stationary fashion, is focused approximately to 0.6 of its initial cross section over a distance of about  $0.5 L_d$ ,

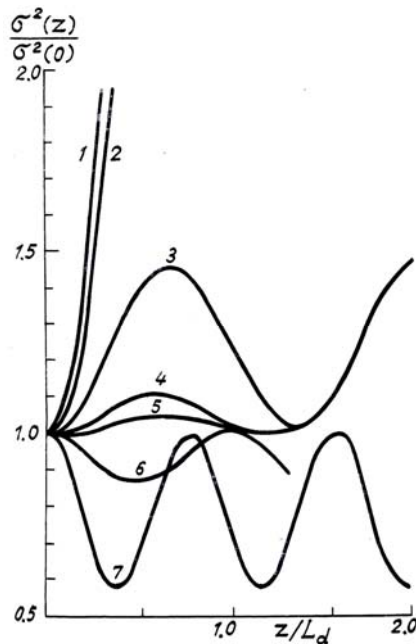


FIG. 1 The behavior of the cross section of a beam in a medium with a gaussian nonuniformity of the refractive index  $R = 0$ :  $\eta_0 = \pi$ ; 1 -  $V = 0$ ; 2 -  $V = \eta_0$ ; 3 -  $V = 2 \eta_0$ ; 4 -  $V = 2.25 \eta_0$ ; 5 -  $V = 2.3 \eta_0$ ; 6 -  $V = 2.5 \eta_0$ ; 7 -  $V = 3 \eta_0$ .

It is interesting to compare the profiles of beams focused approximately to the same value  $\sigma^2(z)$  but for different reasons: owing to an increase in  $V$  at  $R = 0$  and owing to nonlinearity. In Fig. 3 the profile  $|E|$  of maximally focused beams, corresponding to the minima on curve 7 in Fig. 1 and curve 4 in Fig. 2, is compared with the effective gaussian profile. It is obvious that focusing owing to nonlinearity (Fig. 3a) causes a significantly larger deviation of the field profile from the gaussian form than in the case of focusing owing to deepening of the profile of the nonuniformity of a linear medium (Fig. 3b); in addition, the nonlinearity sharpens the profile and increases the energy concentrated in the part of the beam near the axis.

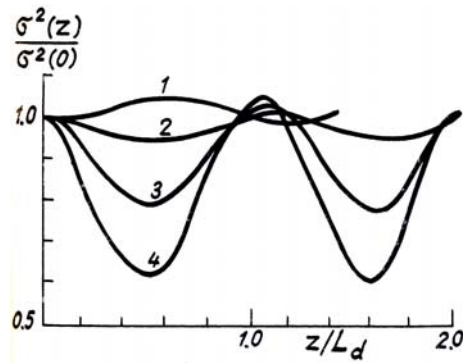


FIG. 2. The effect of nonlinearity on the propagation of a gaussian beam in a nonuniform medium with a gaussian profile of the refractive index:  $\eta_0 = \pi$ ;  $V = 2.3 \eta_0$ ; 1 -  $R = 0$ ; 2 -  $R = 1$ ; 3 -  $R = 3$ ; 4 -  $R = 5$ .

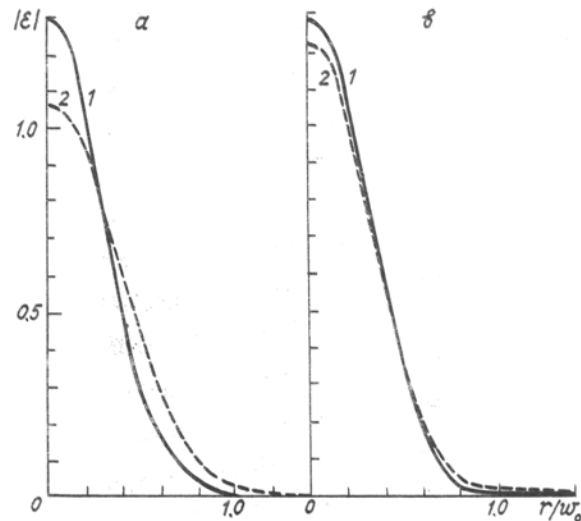


FIG. 3. Deviation of the profile of the modulus of the amplitude of the field from a gaussian form at the points of maximum focusing: a - owing to nonlinearity ( $V = 2.3 \eta_0$ ,  $R = 5$ ); b - owing to nonuniformity of the linear medium ( $V = 3 \eta_0$ ,  $R = 0$ ); 1 - profiles calculated by our method; 2 - effective gaussian profiles.

2. *Nonuniformity with a hypergaussian profile.* Analogous studies were performed for a hypergaussian profile of the refractive index  $V = \exp(-r^6)$  which is closer to a square profile. Figure 4 shows that in the linear regime the growth of  $V$  on the whole leads to the same consequences as in the case of a nonuniform with a gaussian profile. The difference lies in the fact that focusing on the starting segment starts for significantly larger values of  $V$ ,  $V = 4 \eta_0$ , instead of  $V = 2.3 \eta_0$ . Another significant difference is that fine structure appears in the graph of  $\sigma^2(z)$  (curve 3) with almost stationary propagation of the beam. This structure was reproduced in a stable fashion with an

accuracy of not worse than several percent as the step  $\Delta z$  was varied from 0.002 up to 0.005: this removed the initial suspensions that it is related with the numerical error. Analysis of the evolution of the profile  $|E|$  in this case showed that in those sections where  $\sigma^2(z)$  was maximum and equal to the starting value, the profile had a sharp peak and comparatively slowly decaying wings. In those sections where  $\sigma^2(z)$  is minimum the peak of the profile becomes flat (a shallow and very wide dip can occur at the center) and the wings become steep. These features can be explained by the effective excitation of at least the two lowest characteristic modes of the nonuniform medium, and in addition the magnitude and sign of the contribution of the highest of these modes change as a function of  $z$ .

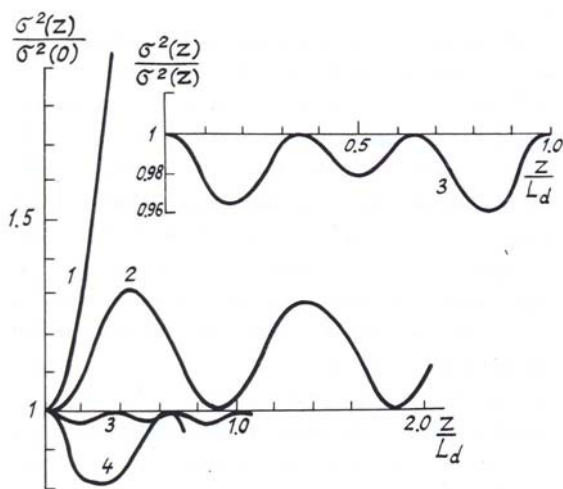


FIG. 4. The linear regime of the propagation of a beam with a gaussian starting profile in a medium with a hypergaussian nonuniformity. The fine structure of curve 3 is shown separately: 1 -  $V = \eta_0$ ; 2 -  $V = 3 \eta_0$ ; 3 -  $V = 4 \eta_0$ ; 4 -  $V = 5 \eta_0$ ,  $R = 0$ .

As in the preceding case, the nonlinearity is manifested as increased focusing of the beam (Fig. 5), and the fine structure described above is smoothed out (transition from curve 1 to curve 4). This can be explained by the effect of the contribution  $N_2 |E|^2$  to the refractive index owing to which the part of the hypergaussian profile of the nonuniformity near the axis becomes less flat; the profile approaches a gaussian profile.

In all of the calculations performed the total power  $W$  which in the absence of losses should be constant was monitored. The drift of  $W$  from its starting value did not exceed several percent.

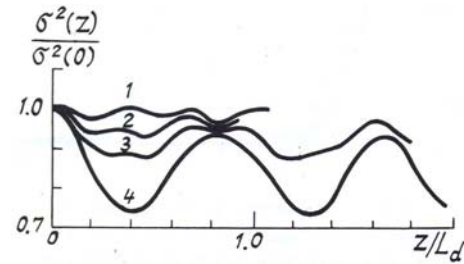


FIG. 5. The effect of nonlinearity on the propagation of a beam in a medium with a nonuniformity having a hypergaussian profile:  $V = 4 \eta_0$ ; 1 -  $R = 0$ ; 2 -  $R = 1$ ; 3 -  $R = 2$ ; 4 -  $R = 4$ .

The results obtained indicate that the cubic nonlinearity strongly affects the propagation of a gaussian beam in an axisymmetric nonuniform medium. They also demonstrate that the computational algorithm which we developed can be effectively employed for modeling the propagation of light beams in nonlinear nonuniform media of different nature, in particular, in problems of laser sounding of the atmosphere and atmospheric optics.

We are grateful to L.A. Mel'nikov for useful discussions and A.D. Novikov for assistance in the computer calculations.

## REFERENCES

1. V.M. Volkov and V.V. Drits, *Differential Methods of Solving Some Problems in Nonlinear Optics*. Institute of Mathematics of the Academy of Sciences of the USSR, No. 31/301, **23** (1987).
2. A.A. Afanasiev, V.M. Volkov, V.V. Drits, and B.A. Samson, *Numerical Method of Calculating the Two-Wave Interaction of Light Pulses Accompanying their Propagation through Nonlinear Media*, Institute of Mathematics of the Academy of Sciences of the USSR, No. 28/298, **22** (1987).
3. A.F. Siegman, *Opt. Letters.*, **1**, No. 1, 13 (1977).
4. C. Bardin et al., *Proc. Soc. Photo-Opt. Instrum. Eng.*, **540**, 581 (1985).
5. V.A. Vysloukh and T.A. Matveeva, *Izv. Vyssh. Uchebn. Zaved, Ser. Radiofiz.*, **28**, No. 1, 101 (1985).
6. A.B. Igumnov, A.S. Solov'ev, and N.N. Yanenko, *Numerical Investigation of Wave Phenomena in Nonlinear Media with Dispersion*, Preprint Institute of Theoretical and Applied Mechanics of Siberian Branch of Academy of Sciences of the USSR, No. 25-83, 15 (1983).
7. G. Bateman and A. Erdelyi, *Higher Transcendental Functions* (Moscow, Nauka, 1966).